Journal of Power Sources 216 (2012) 269–272

Contents lists available at SciVerse ScienceDirect

Journal of Power Sources

journal homepage: www.elsevier.com/locate/jpowsour

Short communication

Magnetic-field effect on dye-sensitized ZnO nanorods-based solar cells

Fengshi Cai [a,b], Jing Wang [a], Zhihao Yuan [a,b,c,*], Yueqin Duan [a,c]

[a] Nanomaterial & Nanotechnology Research Center, Tianjin University of Technology, Tianjin 300384, PR China
[b] Key Laboratory of Display Materials and Photoelectric Devices, Tianjin University of Technology, Ministry of Education of China, Tianjin 300384, PR China
[c] Tianjin Key Lab for Photoelectric Materials & Devices, Tianjin 300384, PR China

HIGHLIGHTS

- The effect of a magnetic field on the photovoltaic performance was investigated.
- Photocurrent was enhanced at magnetic fields of less than 10 mT.
- Applied magnetic field increased the efficient separation of electron–hole pairs.

ARTICLE INFO

Article history:
Received 6 March 2012
Received in revised form
30 April 2012
Accepted 17 May 2012
Available online 1 June 2012

Keywords:
Dye-sensitized solar cells
Magnetic-field
Zinc oxide nanorods
Photovoltaic performance

ABSTRACT

We reported on the effect of an external magnetic field on the photovoltaic performance of Ru-bipyridyl dye N719 or CdS-sensitized ZnO nanorods-based solar cells (DSCs). At the short circuit, increases in photocurrent of ~25% and ~34% can be obtained at an external magnetic fields of less than 10 mT for N719 and CdS-DSCs, respectively, which in turn increase the energy conversion efficiency of ~31% and ~46%. This increase in photocurrent is attributed to an increase in the efficient separation of electron–hole pairs and a decrease in electron transport resistance in ZnO nanorods film under applied magnetic field. These interesting magnetic-field effects can lead to new potential applications in enhanced DSCs efficiency.

1. Introduction

ZnO-based dye-sensitized solar cells (DSCs) have attracted considerable interest due to its higher carrier mobility and simple fabrication [1]. However, overall solar-to-electric energy conversion efficiency of ZnO-based DSCs is still relatively low [2–4]. Over this period, attentions have been focused on improving the efficiency of ZnO-based DSCs using nanostructured ZnO materials and surface treatments [5–8]. The basic electron transfer processes in DSCs consists of the generation, recombination and migration of photo-induced carrier in semiconductors/dye/electrolyte interface [9–12]. During these processes, the efficient separation of electron and hole plays a significant role in enhancing device efficiency [13,14]. The primary charge separation step in DSCs comprises electron injection from the dye excited state into the ZnO conduction band and concomitant hole injection into the redox electrolyte, resulting in a spatial separation of electrons and holes. However, the dye excited state can be potentially quenched by either oxidative or reductive quenching in the presence of the redox couple, and this may be a significant factor influencing DSCs device performance [15,16]. Improved injection performance in DSCs based on the Ru black dye have been reported to be effected by employed electrolyte additives such as lithium ions and tert-butylpyridine [17,18].

Recently, the effect of magnetic fields on the efficiency and current in the organic light emitting diode and organic photovoltaic devices has been receiving increasing interest [19]. It is noted that the generation of charge carriers from photoexcited states is sensitive to the external magnetic field, which may modify the singlet and triplet ratios of the organic semiconductor by perturbing the electron and hole precessions during e–h recombination. Therefore, an external magnetic field can, in principle, change photocurrent by varying the injection performance and charge transport resistance involved in excited processes and charge transport. However, the influence of such external magnetic field upon the photocurrent of DSCs, and their correlation with device performance, has received only limited attention to date. In the

* Corresponding author. Nanomaterial & Nanotechnology Research Center, Tianjin University of Technology, Tianjin 300384, PR China. Tel./fax: +86 22 60214019.
E-mail address: zhyuan@tjut.edu.cn (Z. Yuan).

0378-7753/$ – see front matter © 2012 Elsevier B.V. All rights reserved.
doi:10.1016/j.jpowsour.2012.05.042

present works, we report the results of preliminary measurements of the effect of a magnetic field on the photovoltaic performance of ZnO-based DSCs. We found that the effect of an external magnetic field as low as 10 mT is sufficient to increase the photocurrent in the ZnO-based DSCs.

2. Experimental section

2.1. Preparation of the ZnO nanorod electrode

ZnO nanorods arrays were grown on ZnO-seeded fluorinated tin oxide (FTO) (15 Ω per square, Nippon Sheet Glass) substrates by chemical bath deposition. The ZnO seed layer was prepared by sol–gel method as described in Ref. [9]. The ZnO seed solution was spin-coated onto FTO glass substrates, and then dried in an oven at 60 °C for 30 min. The ZnO seed substrates were then immersed in an aqueous solution of 0.05 M zinc nitrate hydrate and 0.05 M hexamethylenetetramine at 95 °C to grow ZnO nanorods. The synthesis solution was replaced with fresh solution every 3 h to achieve sufficiently long nanorods. The nanorod arrays were then rinsed with deionized water and dried at room temperature. To modify the surface condition and crystallinity of ZnO nanorods, a post-thermal treatment was performed on ZnO nanorod samples at 300 °C for 1 h in the air.

2.2. Assembly of the DSCs

For DSCs fabrication, ZnO nanorods based electrodes were immersed in a 0.3 mM ethanol solution of N719 at room temperature for overnight for dye loading. The dye adsorbed ZnO film electrodes were then rinsed with ethanol and dried under a nitrogen stream. In addition, the CdS-sensitized ZnO nanorods electrode was prepared by immersing ZnO nanorod into the aqueous solution consisting of 0.01 M $Cd(NO_3)$, 0.01 M Na_2S at 60 °C for 10 min. The Pt counter electrode was prepared by thermal decomposition of H_2PtCl_6 (0.03 M in isopropanol) on FTO at 380 °C for 30 min. The two electrodes were clipped together, and used a thermoplastic film (60 μm in thickness, Dupont, Surlyn 1702) as sealant to prevent the electrolyte solution from leaking. The composition of the iodide/triiodide (I^-/I_3^-) electrolyte is 0.6 M 1-butyl-3-methyl imidazolium iodide (BMII), 0.03 M iodine, 0.1 M guanidinium isothiocyanate, 0.5 M 4-tert-butylpyridine in acetonitrile. The active electrode area is 0.16 cm^2.

2.3. Characterization and measurements

The morphologies and microstructures of the ZnO nanorods films were characterized by scanning electron microscope (SEM, JEOL, JSM-6700F, 10 kV). To measure the effect of magnetic fields the sample was placed between the poles of an electromagnet and was measured under repeating the applied magnetic field and null magnetic field conditions, as shown in Fig. 1. The axial direction of the nanowire was perpendicular to the magnetic field. The intensity of magnetic field was measured by teslameter (model SG-4L). The photocurrent–voltage characteristics of the cells were recorded using a Keithley model 2400 digital source meter (Keithley Instruments Inc., USA) at room temperature. An AM 1.5 solar simulator - Oriel 91160–1000 with a 300 W Xe lamp was used as the light source. The incident-light intensity was calibrated to 100 mW cm^{-2} using a standard single-crystal Si solar cell. The light-to-electricity conversion efficiency (η) of the DSCs is calculated from the short-circuit photocurrent density (J_{sc}), the open-circuit photovoltage (V_{oc}), the fill factor of the cell (ff), and the intensity of the incident light (I_s) by the following equation [20]:

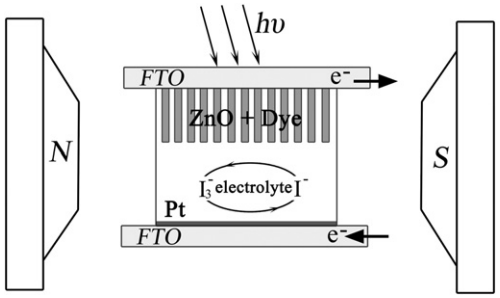

Fig. 1. Schematic of a dye-sensitized solar cells under external magnetic field.

$$\eta = \frac{J_{sc}V_{oc}ff}{I_s}$$

The electrochemical performance was investigated by means of a PARSTAT 2273 instrument at open-circuit potential under AM 1.5 one sun light illumination, with frequency range of 0.01–10^5 Hz. The magnitude of the alternative signal was 10 mV. The electrical impedance spectra were analyzed using Z-View software.

3. Results and discussion

Fig. 2 is the SEM images of the ZnO nanorods formed after reaction time for 9 h. The SEM image in Fig. 2(a) shows the top view of ZnO nanorods film. The typical diameters of these individual ZnO nanorods are in the range of 50–100 nm. Fig. 2(b) shows a cross

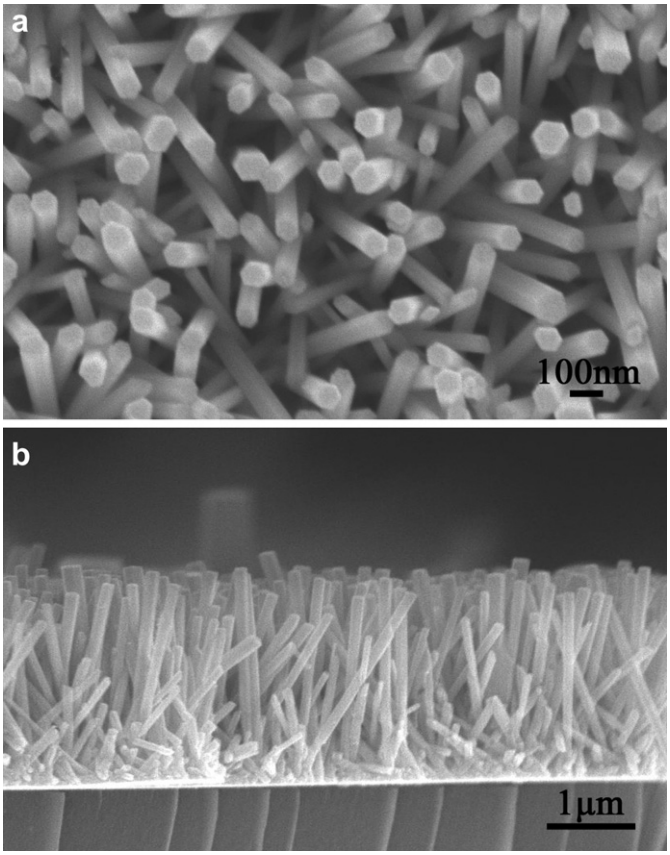

Fig. 2. (a) Top view and (b) cross-sectional SEM images of the ZnO nanorods. The nanorods growth time is 9 h.

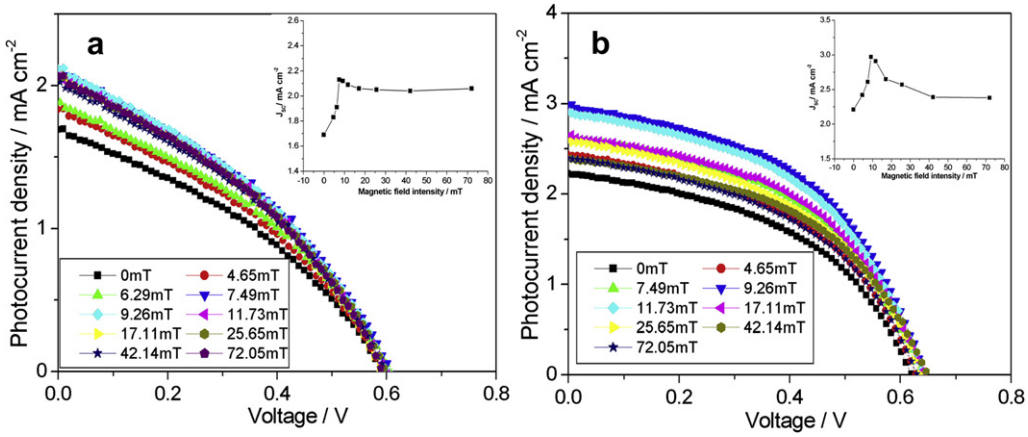

Fig. 3. Photocurrent–photovoltage characteristics of N719 (a) or CdS (b) sensitized ZnO nanorods solar cells under different magnetic field intensity. The inset shows the change of short circuit photocurrent density as a function of magnetic field intensity.

section of the ZnO film structure. The ZnO thickness is about 2.4 μm. It also can be seen that the hexagonal nanorods uniformly covered the substrate and grew vertically on the seed layer with uniform sizes and lengths, providing an efficient electron transition channel when assembled to a dye sensitized solar cell.

Fig. 3 shows the photocurrent–photovoltage characteristics of N719 or CdS sensitized ZnO nanorods solar cells at different magnetic field intensity (B). The changes of J_{sc}, V_{oc}, *ff*, and η for both the N719 and CdS-based cells as a function of magnetic field intensity are depicted in Fig. S3. It can be seen that the change trend of the photovoltaic performance parameters for both the N719 and CdS-based cells is similar. As shown in Fig. 3 and Fig. S3, the J_{sc} and η steeply increase with increasing *B* in the low field range of less than 10 mT and reaches up to maximum, while the V_{oc} and ff are no notable change. For the N719 dye, the J_{sc} and η are enhanced moderately from 1.69 to 2.13 mA cm^{-2} and 0.36–0.47% at low magnetic field (<10 mT) and then become nearly constant at high magnetic field (>20 mT), respectively. The same behavior is observed for the CdS sensitizer, where application of a low field range of less than 10 mT produces a clear increase in the J_{sc} from 2.21 to 2.97 mA cm^{-2} and the η from 0.63 to 0.92%, and then produces a slow decreases at high magnetic field (>20 mT). It can be seen that the effect of the external magnetic field on increasing the photocurrent and efficiency in the device is clear. To confirm the validity of the observed data, the sample was measured under repeating the applied magnetic field and null field conditions. The reproducibility indicates good device stability (see Supporting Information Fig. S2).

To analyze the effect of an external magnetic field on the charge transport properties in DSCs, electrochemical impedance spectroscopy (EIS) was done. Fig. 4a shows the typical impedance spectra changing as a function of magnetic field intensity for the ZnO nanorods solar cells sensitized by N719. The impedance spectra for CdS sensitized ZnO solar cells are shown in Fig. S4. Two semicircles, including a small one at high frequency and a large semicircle at low frequency, are observed in the Nyquist plots of EIS spectra (see Fig. 4a). The small semicircle in the high frequency range is assigned to the impedance related to charge transport at the Pt electrode/electrolyte interface (R_c) [21,22]. The large semicircle in the low-frequency region fitted to an electron transport resistance (R_d), a charge-transfer resistance (R_{ct}) and a chemical capacitance (C_μ) represents the accumulation/transport of the injected electrons within ZnO film and the charge transfer across either the ZnO/redox electrolyte interface or the FTO/ZnO interface.

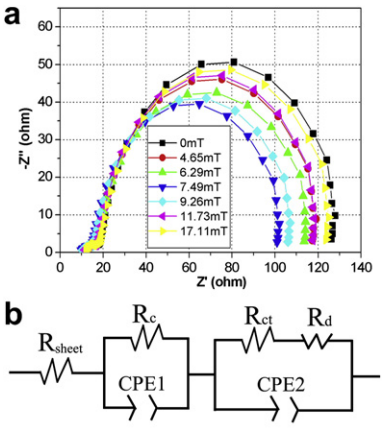

Fig. 4. (a) Nyquist plots for N719-DSCs with different magnetic field intensity. (b) Equivalent circuit for the impedance spectrum. R_d: electron transport resistance; R_{ct}: charge-transfer resistance; C_μ: chemical capacitance; R_{sheet}: serial resistance.

According to the EIS model reported in the literature [22], the fitting parameters including R_d and R_{ct} obtained by Zsimpwin software are exhibited in Table 1. It can be seen that the R_{ct} and R_d decreased with an increase in low magnetic field intensity. The similar behavior is also observed in the CdS sensitized cell. Furthermore, the effective lifetime of electrons (τ_{eff}) is determined by peak frequency (ω_{max}) value of the central arc, where $\tau_{eff} = 1/\omega_{max}$ [23], yielding 0.023 s for the N719-DSCs under magnetic field (7.49 mT). In comparison, the τ_{eff} for the N719-DSCs under magnetic field (0 mT) is 0.015 s. These results suggest that applying an external magnetic field can increase the electron density and the

Table 1
Impedance parameters of R_{ct} and R_d of N719-DSCs with different magnetic field intensity estimated from the impedance spectra in Fig. 4.

B (mT)	R_{ct} (Ω)	R_d (Ω)	τ_{eff} (s)
0	108.6	34.2	0.015
4.65	96.3	30.4	0.017
6.29	93.5	29.6	0.018
7.49	82.1	25.3	0.023
9.26	87.9	27.3	0.020
11.73	96.8	30.2	0.018
17.11	102.7	32.9	0.017

electron lifetime, thus contributing to the small R_{ct} and R_d and the increase of the J_{sc} [23].

Based on the above photocurrent–voltage characteristics and electrochemical impedance properties, we discuss the origin of the magnetic field effect in the ZnO-based DSCs. Photocurrent generation in DSCs results from four sequential processes: light absorption, formation of excited states, generation of charge carriers from photoexcited states, and transport of charge carriers in semiconducting materials. For DSCs based on the Ru-based dye, strong spin-orbit coupling from the ruthenium heavy atom center accelerates intersystem crossing, resulting in an additional injection mechanism proceeding via the lower energy triplet excited state [12]. Previous studies have indicated that it is much easier to achieve efficient electron injection from the triplet rather than the singlet state of the ruthenium-based dye [24].

It is noted that an external magnetic field can perturb the electron and hole precession rates, leading to the redistribution of singlet and triplet populations [19]. Thus, an external magnetic field can, in principle, change photocurrent by varying the singlet and triplet ratios involved in excited processes and charge transport. As a consequence, the photocurrent plots show a sharp rise at magnetic field up to ~10 mT, followed by a saturation regime for increasing magnetic field in our experiments. Hence, the increase in photocurrent and overall light conversion efficiency observed in the low magnetic field is ascribable to the hyperfine mechanism (HFM) [25], which arises from an increase in the population of triplet states relative to singlets and thereby increases the efficiency of charge separation. The decrease of the photocurrent at magnetic field (>20 mT) may result from a saturation in intersystem crossing and an increase of charge transport resistance in ZnO film with applied magnetic field. Further studies of the effect of an external magnetic field on the photovoltaic performance are in progress.

4. Conclusions

In conclusion, we have observed that a modest external magnetic field can increase the photocurrent, conversion efficiency of DSCs. When the external magnetic field (B) of 10 mT is applied, the J_{sc} and the η of N719-DSCs increase from 1.69 to 2.13 mA cm^{-2} and from 0.36 to 0.47%, while the value of J_{sc} and η increase from 2.21 to 2.97 mA cm^{-2} and from 0.63 to 0.92% for CdS-DSCs. Electrochemical measurements show that applied magnetic field increases the efficient separation of electron–hole pairs and reduces electron transport resistance of DSCs. Thus we believe that the application of magnetic field has the potential to improve the photovoltaic response significantly.

Acknowledgments

This work was supported by the National NSFC (20903073, 50872092) and Tianjin Natural Science Foundation (09JCYBJC07000).

Appendix A. Supporting Information

Supplementary material associated with this article can be found, in the online version, at doi:10.1016/j.jpowsour.2012.05.042.

References

[1] Q.F. Zhang, C.S. Dandeneau, X.Y. Zhou, G.Z. Cao, Adv. Mater. 21 (2009) 1–22.
[2] K. Keis, J. Lindgren, S.E. Lindquist, A. Hagfeldt, Langmuir 16 (2000) 4688–4694.
[3] H. Horiuchi, R. Katoh, K. Hara, M. Yanagida, J. Phys. Chem. B 107 (2003) 2570–2574.
[4] A.B.F. Martinson, J.W. Elam, J.T. Hupp, M.J. Pellin, Nano Lett. 7 (2007) 2183–2187.
[5] K. Kakiuchi, E. Hosono, S. Fujihara, J. Photochem. Photobiol. A 179 (2006) 81–86.
[6] T.R. Zhang, W.J. Dong, M. Keeter-Brewer, S. Konar, J. Am. Chem. Soc. 128 (2006) 10960–10968.
[7] L.J. Luo, W. Tao, X.Y. Hu, T. Xiao, B.J. Heng, W. Huang, H. Wang, H.W. Han, Q.K. Jiang, J.B. Wang, Y.W. Tang, J. Power Sources 196 (2011) 10518–10525.
[8] T.B. Guo, Y.Q. Chen, L.Z. Liu, Y.F. Cheng, X.H. Zhang, Q. Li, M.Q. Wei, B.J. Ma, J. Power Sources 201 (2012) 408–412.
[9] M. Law, L.E. Greene, J.C. Johnson, P.D. Yang, Nat. Mater. 4 (2005) 455–459.
[10] Y.J. Lee, D.S. Ruby, D.W. Peters, Nano Lett. 8 (2008) 1501–1505.
[11] T.W. Hamann, J.W. Elam, M.J. Pellin, J.T. Hupp, Adv. Mater. 20 (2008) 1560–1564.
[12] A. Listorti, B. O'Regan, J. R Durrant, Chem. Mater. 23 (2011) 3381–3399.
[13] F. Ito, T. Ikoma, J. Phys. Chem. B 109 (2005) 7208–7213.
[14] T. Iimori, T. Nakabayashi, J. Phys. Chem. A 112 (2008) 4432–4436.
[15] P. Wang, B. Wenger, R. Humphry-Baker, J.E. Moser, J. Teuscher, W. Kantlehner, J. Mezger, E.V. Stoyanov, S.M. Zakeeruddin, M. Grätzel, J. Am. Chem. Soc. 127 (2005) 6850–6856.
[16] T. Dos Santos, A. Morandeira, S. Koops, A.J. Mozer, G. Tsekouras, Y. Dong, P. Wagner, G. Wallace, J.C. Earles, K.C. Gordon, D. Officer, J.R. Durrant, J. Phys. Chem. C 114 (2010) 3276–3279.
[17] Z.S. Wang, T. Yamaguchi, H. Sugihara, H. Arakawa, Langmuir 21 (2005) 4272–4276.
[18] D.F. Watson, G.J. Meyer, Coord. Chem. Rev. 248 (2004) 1391–1406.
[19] B. Hu, L. Yan, M. Shao, Adv. Mater. 21 (2009) 1500–1516.
[20] A. Hagfeldt, M. Grätzel, Acc. Chem. Res. 33 (2000) 269–277.
[21] J. Bisquert, J. Phys. Chem. B 106 (2002) 325–333.
[22] F. Fabregat-Santiago, J. Bisquert, E. Palomares, L. Otero, D.B. Kuang, S.M. Zakeeruddin, M. Grätzel, J. Phys. Chem. C 111 (2007) 6550–6560.
[23] M. Adachi, M. Sakamoto, J.T. Jiu, Y. Ogata, S.J. Isoda, J. Phys. Chem. B 110 (2006) 13872–13880.
[24] A. Morandeira, I. Lopez-Duarte, M.V. Martinez-Diaz, B. O'Regan, C. Shuttle, N.A. Haji-Zainulabidin, T. Torres, E. Palomares, J.R. Durrant, J. Am. Chem. Soc.sb:maintitle> 129 (2007) 9250–9251.
[25] U.E. Steiner, T. Ulrich, Chem. Rev. 89 (1989) 51–147.